

- ¹H. S. W. Massey and C. BO. Mohr, Proc. Roy. Soc. (London) A136, 289 (1932).
- ²R. Ra. Damburg and M. Gailitis, Proc. Phys. Soc. (London) 82, 1068 (1963).
- ³P. G. Burke, D. F. Gallaher, and S. Geltman, J. Phys. B 2, 1142 (1969).
- ⁴A. R. Holt and B. L. Moiseiwitsch, J. Phys. B 1, 36 (1968).
- ⁵L. A. Vainshtein, L. Presnyakov, and I. Sobelman, Zh. Eksperim. i Teor. Fiz. 45, 2015 (1963)[Sov. Phys. JETP 18, 1383 (1964)].
- ⁶V. I. Ochkur, Zh. Eksperim. i Teor. Fiz. 45, 734 (1963) [Sov. Phys. JETP 18, 503 (1964)].
- ⁷S. N. Banerjee, R. Jha, and N. C. Sil, Indian J. Phys. 40, 489 (1966).
- ⁸A. Temkin, Phys. Rev. 116, 353 (1959).
- ⁹R. J. Glauber, in *Lectures in Theoretical Physics*, edited by W. E. Brittin *et al.* (Interscience, New York, 1959), Vol. 1, p. 315.
- ¹⁰A. S. Ghosh and N. C. Sil, Indian J. Phys. 44, 153 (1970).
- ¹¹L. D. Faddeev, Zh. Eksperim. i Teor. Fiz. 39, 1459 (1960) [Sov. Phys. JETP 12, 1014 (1961)].
- ¹²C. Lovelace, Phys. Rev. 135, B1225 (1964).
- ¹³A. Ahmedzadeh and J. A. Tjon, Phys. Rev. 139, B1085 (1965).
- ¹⁴O. E. Alt, P. Grassberger, and W. Sanhas, Nucl. Phys. B2, 167 (1967).
- ¹⁵James S. Ball, Joseph C. Y. Chen, and D. Y. Wong, Phys. Rev. 173, 202 (1968).
- ¹⁶Joseph C. Y. Chen, K. T. Chung, and P. J. Kramer, Phys. Rev. 184, 64 (1969).
- ¹⁷I. H. Sloan and E. J. Moore, J. Phys. B 1, 414 (1968).
- ¹⁸M. J. Seaton, Proc. Phys. Soc. (London) 77, 174 (1961).
- ¹⁹N. F. Mott and H. S. W. Massey, *The Theory of Atomic Collisions*, 3rd ed. (Clarendon, London, 1968), p. 547.
- ²⁰R. H. Neynaber, L. L. Marina, E. W. Rothe, and S. M. Trujillo, Phys. Rev. 124, 135 (1961).
- ²¹P. G. Burke, H. M. Schey, and K. Smith, Phys. Rev. 129, 1258 (1963).
- ²²Peak values obtained in different approximations are as follows: (i) distorted wave (Ref. 25): 0.709; (ii) cc approximation (Ref. 21): 0.36; (iii) FBA approximation: 0.245; (iv) present approximation: 0.66; (v) BO approximation: too high.
- ²³L. A. Vainshtein, Opti. i Spektroskopiya 11, 301 (1961) [Opt. Spectry. USSR 11, 163 (1961)].
- ²⁴B. L. Moiseiwitsch and J. J. Smith, Rev. Mod. Phys. 40, 337 (1968).
- ²⁵For details regarding the justifications and validity of these approximations, one can see the following references in addition to Ref. 17: Ian H. Sloan, Phys. Rev. 165, 1587 (1968); 185, 1361 (1969).
- ²⁶E. Corinaldesi and L. Trainer, Nuovo Cimento 9, 940 (1952).
- ²⁷P. M. Morse and H. Feshbach, *Methods of Theoretical Physics* (McGraw-Hill, New York, 1953), p. 1082.

Impact-Parameter Dependence of X-Ray Production in Collisions between Energetic Heavy Ions and Atoms

H. J. Stein, H. O. Lutz, P. H. Mokler, and P. Armbruster*

Kernforschungsanlage Juelich, Juelich, Germany

(Received 13 December 1971)

18- to 46-MeV ^{53}I ions were scattered by thin ^{52}Te targets. The L x rays produced in the nearly identical particles ^{53}I and ^{52}Te were measured in coincidence with the scattered I ions. The differential cross section for L x-ray emission shows a maximum at impact parameters comparable to the L -shell radii. For the ion energies E investigated, the total cross section for L x-ray emission in I and Te was found to be proportional to $E^{0.8}$. The results are discussed and compared with theoretical models for inner-shell excitation.

I. INTRODUCTION

In collisions between swift charged particles (electrons, protons, α particles, heavy ions) and atoms vacancies in inner electron shells may be produced. These vacancies are filled by electrons from higher shells via radiative or nonradiative (Auger) transitions. The fraction of radiative transitions is given by the fluorescence yield ω . The corresponding transition probability is strongly dependent on the nuclear charge Z , and dominates in inner shells of heavy atoms.

Atomic collisions can be characterized by a pa-

rameter $\eta = (v/u)^2$, where v is the relative velocity of the collision partners and u the orbital velocity of the electrons in the shell being excited.¹ In the high-velocity limit, $\eta \gg 1$, the excitation and ionization cross section can be calculated by a simple perturbation treatment (e. g., Born approximation, cf. Refs. 1 and 2). In contrast to electron scattering, excitation and ionization in collisions between atomic particles are still possible in the "quasiadiabatic" velocity region, $\eta < 1$. Here, the calculation is generally more difficult. Under certain conditions, a simple perturbation treatment as in the high velocity limit is sufficient: if $Z_1 \ll Z_2$,

the perturbation of the wave function of the bound atomic electron is small; in case of small deflections of the primary, Born approximation can be applied.³ For this case, the equivalence of the plane-wave Born approximation with a semiclassical time-dependent perturbation treatment in impact-parameter approximation was shown by Bang and Hansteen.⁴

This treatment has the advantage that the impact-parameter dependence of excitation and ionization is obtained. Deviations from the impact-parameter approximation (deflection of the incident particle in the Coulomb field of the target atom) can be included in the calculation. The *K*-shell ionization (and to a lesser extent the *L*- and *M*-shell ionization) of various elements ($10 < Z_2 < 80$) has been investigated experimentally in great detail for the quasiadiabatic case.^{2,5-8} For *K*-shell excitation, the agreement between experiment and theory²⁻⁴ is satisfactory. An excellent fit is achieved if the Coulomb deflection and the increase in binding energy of the atomic electron by the presence of the projectile Z_1 is taken into account.⁹

In collision systems $Z_1 \approx Z_2$ and $\eta < 1$, however, a simple perturbation treatment is not valid anymore. In this region, the experimentally determined cross sections are generally too high by orders of magnitude if compared to the theoretical values.¹⁰⁻¹³ *L*-shell ionization of heavy atoms was first studied systematically by Specht.¹⁴ This work was a continuation of investigations by Armbruster¹⁵ using a large variety of ion-atom combinations. The projectiles were "light" and "heavy" fission fragments from ²³⁵U. The *L* ionization cross section showed fluctuations as a function of the nuclear charge Z_2 . Characteristic maxima occur if the *L* binding energies of the projectiles coincide approximately with the *K*, *L*, or *M* binding energies of the target atoms. These maxima were accounted for by the reduction in effective electron binding energy in the "quasimolecule" which is formed in the collision. More recently, similar fluctuations in x-ray emission have been observed for other collision systems.¹⁶⁻¹⁸

For $\eta \ll 1$ and identical collision partners, Fano and Lichten¹⁹ developed a model in which the inner-shell vacancy production is caused by an "electron-promotion" mechanism. This model is based on the well-known concepts of molecular physics, since for $\eta \ll 1$ the electronic motion can adjust adiabatically to the nuclear motion. Excitation is caused by a transition of an electron to an unoccupied higher level at a certain critical internuclear distance (e. g., where two molecular energy levels approach closely). On separation of the two nuclei, the electron has a chance of remaining in the higher level, resulting in an inner-shell vacancy. This model gives a qualitative account of inner-shell excitation

in the case $\eta \ll 1$. Since it involves a semiclassical treatment with well-defined nuclear trajectories, the impact-parameter dependence of the corresponding cross sections may again be obtained explicitly. From this model certain features may be expected and tested experimentally as, e. g., large cross sections and critical transition distances in the order of shell dimensions.

To obtain a more detailed knowledge of the mechanisms involved in inner-shell vacancy production, we studied the impact-parameter dependence of *L* x-ray production in "slow" collisions ($\eta < 1$) of I ions with Te atoms.

II. PRINCIPLE OF PROCEDURE

The x-ray production P_x can be characterized by the collisionally induced x rays measured in coincidence with ions scattered in a single event by a thin target,

$$P_x(\vartheta) = N_x(\vartheta)/N_s(\vartheta), \quad (1)$$

where $N_s(\vartheta)$ is the number of ions scattered through the angle ϑ , and $N_x(\vartheta)$ is the number of coincident *L* x rays.

Transformation of the laboratory scattering angle ϑ into the impact parameter ρ yields $P_x(\rho)$. This transformation may be performed using a classical calculation. If the total inelastic energy loss Q in the collision is small compared to the primary energy E , the ϑ, ρ relationship can be calculated from the elastic-scattering law. The scattering angle θ in the center-of-mass system is given by

$$\theta = \pi - 2 \int_{r_0}^{\infty} \frac{\rho dr}{r^2 [1 - V(r)/E_{\text{rel}} - \rho^2/r^2]^{1/2}}, \quad (2)$$

where $E_{\text{rel}} = v^2 m_1 m_2 / 2(m_1 + m_2)$ is the relative energy of the particles with masses m_1 and m_2 , r is the internuclear distance, and r_0 is the distance of closest approach for a given impact parameter ρ . The laboratory scattering angle ϑ can be calculated from the center-of-mass scattering angle θ :

$$\tan \vartheta = (m_2 \sin \theta) / (m_1 + m_2 \cos \theta). \quad (3)$$

For the scattering system I-Te (mean masses 127 and 127.6, respectively), $\vartheta = \frac{1}{2}\theta$. The scattering potential used was a screened Coulomb potential:

$$V(r) = (Z_1 Z_2 e^2 / r) e^{-r/a}, \quad (4)$$

where the screening length $a = a_0 (Z_1^{2/3} + Z_2^{2/3})^{-1/2}$, with $a_0 = 0.529 \times 10^{-8}$ cm.²⁰ The scattering integral (2) can be solved numerically using a method given in Ref. 21. Throughout the paper, the impact parameter ρ is used as the characteristic collision parameter. In the system investigated, it is practically equal to the distance of closest approach r_0 , except at the smallest ρ (cf. Fig. 5).

The total x-ray production cross section may be

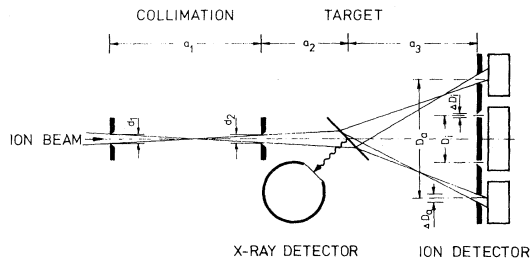


FIG. 1. Schematic of experimental setup. The characteristic dimensions were (in mm) $a_1=2820$, $a_2=295$, $a_3=123, \dots, 1394$; $D_i=20$, $\Delta D_i=1$, $D_a=63$, $\Delta D_a=3$; $d_1, d_2=1, \dots, 3$.

calculated by integrating the differential cross section $d\sigma_x = 2\pi P_x(\rho)\rho d\rho$ over all impact parameters,

$$\sigma_x(\text{calc}) = 2\pi \int_0^\infty P_x(\rho)\rho d\rho. \quad (5)$$

Additionally, as a cross check, σ_x can be measured directly and compared to the value obtained from the differential scattering experiment,

$$\sigma_x(\text{meas}) = (N_{x,\text{tot}}/N_{s,\text{tot}})/n. \quad (6)$$

$N_{x,\text{tot}}$ is the total number of x rays (corrected for background) induced by the total number $N_{s,\text{tot}}$ of ions transmitted through the thin target, and n is the number of target atoms/cm². No coincidence between $N_{x,\text{tot}}$ and $N_{s,\text{tot}}$ is used in this case.

III. EXPERIMENTAL METHOD

The ion beam from the Heidelberg model EN tandem accelerator was analyzed in a 90° magnet and a 20° electrostatic deflector²² according to energy and charge. After collimation, it is incident on a thin Te target at an angle of 45°, Fig. 1. The I ions scattered in the target were detected in an annular detector (see below). x rays produced in collisions between ions and target atoms were analyzed in a flow-mode proportional counter. This counter is located at an angle of 135° to the beam direction opposite to the target surface.

The emission of L x rays from I and Te as a function of ion scattering angle ϑ was studied using a 20- $\mu\text{g}/\text{cm}^2$ -thick Te target. Ion energies were 18.6, 30.8, and 46.0 MeV. The influence of target thickness was determined with a 50- $\mu\text{g}/\text{cm}^2$ Te target at an ion energy of 30.8 MeV. The total x-ray excitation cross section was measured directly with a 240- $\mu\text{g}/\text{cm}^2$ Te target at the ion energies 18.6, 24.4, 30.8, 38.0, 46.0, 54.8, and 64.3 MeV. The corresponding charges of the incoming ions ranged from 7⁺ to 13⁺.

The Te targets were vacuum evaporated on thin (15 to 20 $\mu\text{g}/\text{cm}^2$) carbon backings. The carbon backings were located in such a way that they did not face the incident ion beam and the x-ray detec-

tor. The target thickness was controlled during evaporation with a quartz monitor and determined to within $\pm 10\%$ by weighing. The absolute thickness of the 240- $\mu\text{g}/\text{cm}^2$ Te target directly enters the determination of the total x-ray cross section $\sigma_x(\text{meas})$.

In the differential scattering experiment, two annular counters were used to record the scattered ions. These counters consisted of an array of surface-barrier detectors. They are located behind two annular apertures centered on the beam axis (Fig. 1). One detector (400 mm²) is used for the inner aperture, and six detectors (300 mm²) cover approximately 50% active area of the outer aperture. The collimation apertures, the target, and the annular ion detectors were optically centered on a common axis which was then aligned parallel to the beam direction. The scattering angle was varied by moving the detector system along the beam axis. The angles covered with the inner ring were 0.4° to 4.6°, with the outer ring 1.3° to 14.7°. For all scattering angles, the primary beam collimation was varied to give a maximum over-all angular uncertainty of 10%.

To determine the total number of iodine ions transmitted through the target, as is necessary in the direct determination of $\sigma_x(\text{meas})$, a 400-mm² heavy-ion detector was mounted directly behind the target, replacing the annular counting system. With this arrangement, ions scattered through angles up to 8° could be detected. Events involving larger scattering angles have a large x-ray excitation probability; however, they are very rare. The number of detected ions were corrected accordingly using the Rutherford scattering law. At the lowest ion energy (18.6 MeV), which is the most serious case, this correction of the total cross section $\sigma_x(\text{meas})$ was 10%.

The x rays were detected in a flow-mode proportional counter with side window subtending a solid angle of $\Omega/4\pi = (2.5 \pm 0.15) \times 10^{-2}$.

The detector efficiency ϵ was $(95 \pm 2) \times 10^{-2}$ for 4-keV x rays, the escape correction $\kappa = 0.94$. The energy resolution was 18% in case of the 6.4-keV line of a ⁵⁷Co source. Care was taken to shield all x rays from the x-ray detector, except those created by the beam in the target.

To process the electronic signals from the x-ray and ion detectors, conventional modules were employed. The electronic setup is sketched schematically in Fig. 2. The coincidences between ion-scattering and x-ray events in the differential scattering experiment were made using a time-to-pulse-height converter and single-channel analyzers. Total and random coincidence spectra were thus recorded simultaneously. This allows a relatively straightforward subtraction of the background; the background is caused by scattering processes which

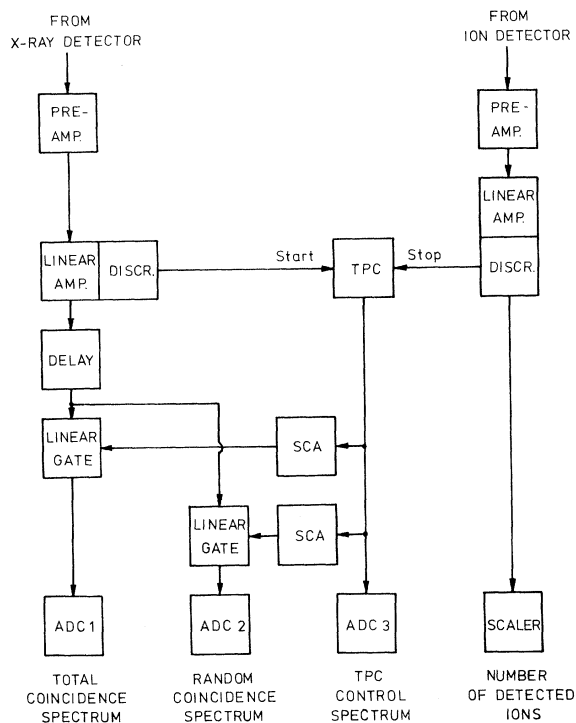


FIG. 2. Schematic of electronic setup. The coincidences between x-ray detector and ion detector signals are made by a time-to-pulse-height converter (TPC) and two timing single-channel analyzers (SCA) to achieve simultaneous recording of total and random coincidences.

are not recorded in the ion detector. It is proportional to the square of the beam intensity, and principally limits the beam intensity.

IV. RESULTS AND ANALYSIS

A typical total x-ray spectrum of the I and Te radiation is shown in Fig. 3. The peak at approxi-

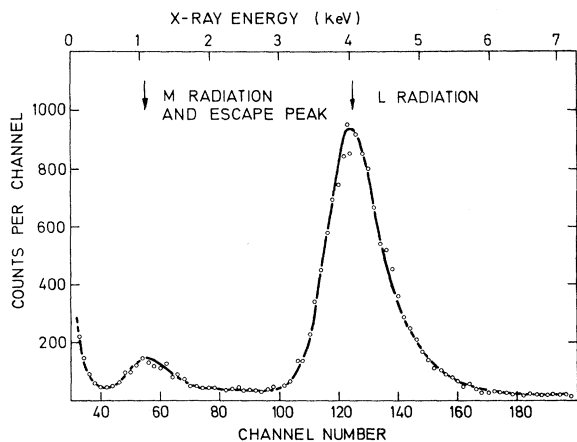


FIG. 3. Total x-ray spectrum from I and Te (240- $\mu\text{g}/\text{cm}^2$ target and 30.8-MeV I energy).

mately 4 keV is caused by the I and Te L radiation. This L line is shifted to higher energies, compared to the photon-induced characteristic radiation.^{14,23-26} The peak at 1 keV comprises the M x rays from I and Te and the escape peak from the L x rays. M radiation is strongly absorbed in the relatively thick window of the x-ray counter. (The transmission is approximately 4% for 1-keV radiation.) In the following we concentrate on the L radiation.

From the total L intensity we get the number of coincident L x rays, $N_x(\theta)$ in Eq. (1), by the expression

$$N_x(\theta) = [\bar{N}_x - \bar{N}_x(\text{random})]/(\kappa\epsilon\Omega/4\pi), \quad (7)$$

where \bar{N}_x and $\bar{N}_x(\text{random})$ are the number of counts in the L lines of the coincident total and random x-ray spectra, respectively; for κ , ϵ , and $\Omega/4\pi$, see above. The x-ray emission was assumed to be isotropic.² The relativistic correction of the solid angle for the radiation emitted by the moving particle varies between 2 and 4% for I-ion energies between 18 and 64 MeV, and is disregarded. The effect of x-ray self-absorption can also be neglected in the 20- and 50- $\mu\text{g}/\text{cm}^2$ Te targets.

The directly measured x-ray production $P_x(\theta)$ for the collision energies 18.6, 30.8, and 46.0 MeV is plotted in Fig. 4. The data were taken with a 20- $\mu\text{g}/\text{cm}^2$ -thick target, except those indicated by open circles, which were taken with a 50- $\mu\text{g}/\text{cm}^2$ target at an ion energy of 30.8 MeV. The deviation of the thicker target data is within the experimental uncertainty except at the smallest scattering angles. This shows that single scattering is predominant in the angular region of importance. The x-ray

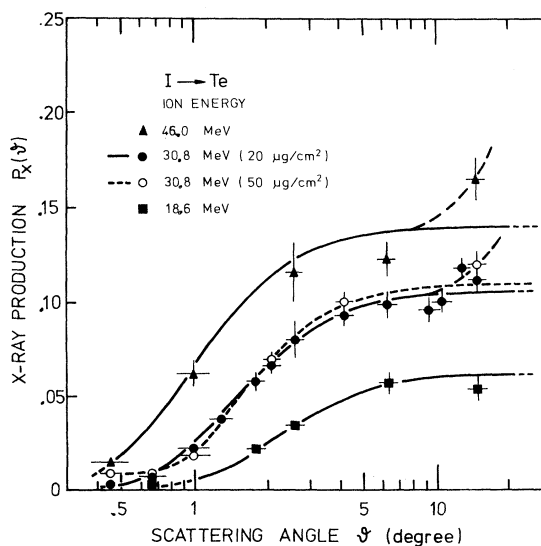


FIG. 4. L x-ray production in the system I-Te as a function of the I scattering angle.

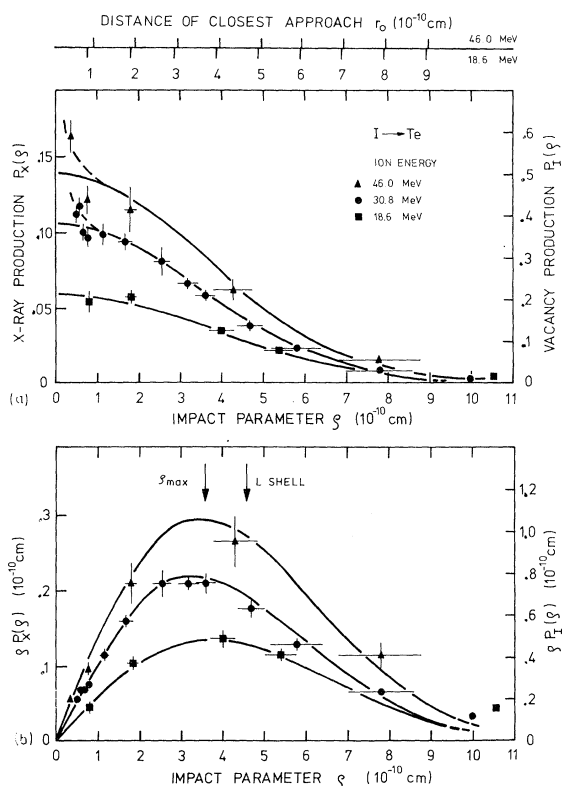


FIG. 5. (a) L x-ray production in the system I-Te (left-hand scale) as a function of the impact parameter. For comparison, the distance of closest approach r_0 is indicated. The right-hand scale gives the L vacancy production in I or Te, assuming equal number of vacancies produced in both particles ($\omega_L = 0.14$). (b) $\rho P_x(\rho)$ as a measure of the differential cross section for L x-ray production; it shows a maximum at ρ values comparable to the L -shell radius.

production increases steeply within a relatively narrow angular region before it flattens out. At high ion energies, a further increase of $P_x(\vartheta)$ may be indicated at large angles.

The transformation of $P_x(\vartheta)$ into $P_x(\rho)$ was performed using Eqs. (2)–(4). $P_x(\rho)$ for the 20- $\mu\text{g}/\text{cm}^2$ Te target is shown in Fig. 5(a), left-hand scale. The right-hand scale gives the vacancy production $P_I(\rho)$ in I or Te, respectively.²⁷ $P_I(\rho)$ is obtained by

$$P_I(\rho) = \frac{1}{2} P_x(\rho) / \omega, \quad (8)$$

where the factor $\frac{1}{2}$ arbitrarily implies that in the practically symmetric system I-Te both collision partners contribute equally to the x-ray emission. A constant fluorescence yield $\omega_L = 0.14$ was assumed; this value is an average for the $L_{I,II,III}$ subshells as obtained by Specht¹⁴ by extrapolating photoexcitation and $K\alpha$ emission experiments. Recent calculations give fluorescence yields which are about a factor of 2 smaller.^{28,29} It should be

noted that $P_I(\rho)$ can only be used as a rough estimate for the vacancy production. The fluorescence yield may strongly be changed in a heavy-ion-atom encounter. Firstly, the excitation of different subshells is not known in the present work; this may give rise to a different average ω_L . Secondly, the degree of ionic excitation and ionization may have a strong influence on the fluorescence yield.^{30,37,38}

The data points in Fig. 5(a) can be fitted empirically with a Gaussian distribution, e. g.,

$$P_I(\rho) = \alpha_I \exp(-\rho^2/2\rho_{max}^2). \quad (9)$$

α_I is the vacancy production in a head-on collision. The additional increase of $P_x(\rho)$ or $P_I(\rho)$ at small impact parameters is indicated by dashed lines.

Figure 5(b) shows $\rho P_x(\rho)$ or $\rho P_I(\rho)$, which is a measure of the differential cross section. It displays a maximum at $\rho_{max} \approx 3.5 \times 10^{-10}$ cm. Within the experimental uncertainty, the position of this maximum is independent of ion energy. It is comparable to the radius of the radial charge-density maximum of the $2p$ state in I or Te (4.3×10^{-10} cm³¹).

The total cross section σ_x or σ_I as a function of ion energy is shown in Fig. 6. $\sigma_x(\text{calc})$, as indicated by squares, is calculated by integrating the curves in Fig. 5(b) over all impact parameters [Eq. (5)]. $\sigma_x(\text{meas})$, as indicated by circles, was measured directly [Eq. (6)]. In the case of the 240- $\mu\text{g}/\text{cm}^2$ Te target the target self-absorption of 4% was taken into account.

The energy dependence of the total cross section can be approximated by $\sigma \propto E^n$, $n = 0.8 \pm 0.1$. This

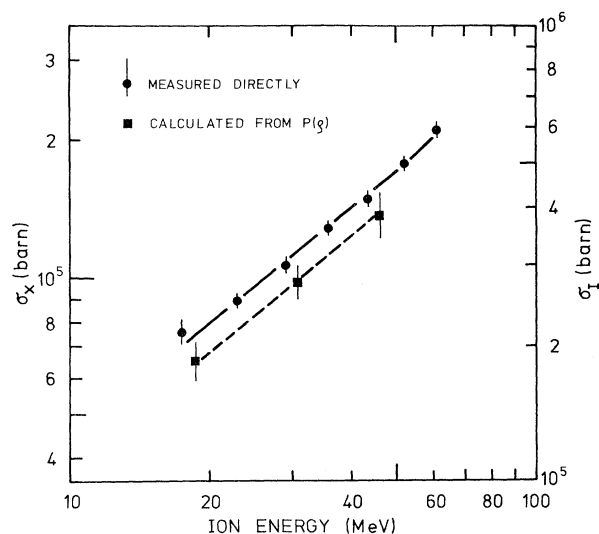


FIG. 6. Total cross section for L x-ray production in the system I-Te (left-hand scale) or L vacancy production in I or Te (right-hand scale, same assumptions as in Fig. 5). The cross-section values as calculated from $P(\rho)$, Fig. 5, and Eq. (5), are in reasonable agreement with the directly measured values.

TABLE I. Widths (FWHM) of the multiple scattering distributions of I ions in a 20- $\mu\text{g}/\text{cm}^2$ Te target on a 15- $\mu\text{g}/\text{cm}^2$ C backing.

Ion energy (MeV)	Width (deg)
18.6	1.07
30.8	0.86
46.0	0.73

energy dependence is roughly determined by the energy dependence of the parameter α_I [Eq. (9)] since ρ_{max} remains nearly constant between 18.6 and 46 MeV. The calculated cross sections are generally somewhat smaller than the cross sections measured directly. Both the measurements of the total and the differential cross section were performed under the same conditions. A discrepancy between $\sigma_x(\text{meas})$ and $\sigma_x(\text{calc})$ can, therefore, only be caused by the interaction potential $V(r)$, which enters the ϑ, ρ transformation, and by a thickness uncertainty in the 240- $\mu\text{g}/\text{cm}^2$ target.

The error bars in Fig. 6 correspond to the statistical uncertainty. The $\sigma_x(\text{calc})$ error bars also include the angular uncertainty. The uncertainty in target thickness only influences $\sigma_x(\text{meas})$. It is indicated separately in the upper left-hand corner of Fig. 6, and acts as a scaling factor. $\sigma_x(\text{calc})$ is independent of any error in target thickness as long as single-collision conditions prevail. A finite target thickness has two effects: (i) A detected ion may have been excited repeatedly in the target; (ii) the scattering angle is altered by multiple scattering of the ions in the target. It can be estimated that the probability for a second L -excitation process in the target is less than 2% for 30.8 MeV and the 20- $\mu\text{g}/\text{cm}^2$ target. Additionally, a comparison between the 50- $\mu\text{g}/\text{cm}^2$ target and the 20- $\mu\text{g}/\text{cm}^2$ target (Fig. 4) shows that the effect (i) can be neglected for all practical purposes. The second effect (ii) can be assessed by using data measured by Rogge.³² The values in Table I give an upper limit for the multiple scattering width of I ions in the 20- $\mu\text{g}/\text{cm}^2$ Te target plus a 15- $\mu\text{g}/\text{cm}^2$ C backing. Unfolding the $P_x(\vartheta)$ curves (20- $\mu\text{g}/\text{cm}^2$ target, Fig. 4) with these multiple scattering distributions shows a slight influence only at $\vartheta < 1^\circ$. For larger angles, the influence is smaller than the statistical error.

In collisions involving small impact parameters, a target atom may be knocked out of the target and detected in the ion counter. These processes give a large x-ray yield. However, they are so rare that their contribution to the experimental results discussed above can be neglected. In addition, the knocked-on target atom can itself give rise to more excitation events in the target. The x rays thus created can cause an increase of the $P_x(\vartheta)$ values,

particularly at large scattering angles ϑ . However, in thin targets the magnitude of this undesired effect is negligibly small: at the largest scattering angles $\vartheta = 14^\circ$, and a primary ion energy of 46 MeV, the knock-on energy is 3 MeV. The total x-ray cross section at an ion energy of 3 MeV is smaller than 6×10^5 b, giving an x-ray yield smaller than 0.006 per knock-on for the 20- $\mu\text{g}/\text{cm}^2$ target. This effect, therefore, cannot play any role in the differential or in the total cross-section measurement reported here.

V. DISCUSSION

The experiment shows that in the system I-Te the large inner-shell excitation cross section is caused by a large geometrical cross section. The bulk of the contribution to the cross section comes from impact parameters around ρ_{max} in the order of L shell dimensions; the maximum ionization α_I occurs at small impact parameters with $\alpha_I < 1$ [Eq. (9)]. The opposite case would be $\rho_{\text{max}} \ll L$ -shell radius and $\alpha_I \gg 1$, a combination which could also give a large cross section. It follows that multiple L -shell excitation is not dominant in the collision system discussed, a result which is also indicated by other experiments.^{24,26} The uncertainty in the fluorescence yield (cf. Sec. IV) cannot alter these conclusions, though it has the effect that the contribution of multiple excitation cannot yet be assessed accurately.

A detailed theoretical description of inner-shell excitation in "slow" collisions between heavy ions and atoms is not available at present. The ion velocities in the cases considered are smaller than the orbital velocities of the L electrons excited ($\eta = 0.15 - 0.3$ for L excitation in I-Te collisions from 18.6 to 46 MeV). The initial atomic wave functions are strongly distorted during the collision, and a quasimolecule with a rotating internuclear axis is formed. Thus, in contrast to excitation by light ions the collision parameters derived in this work (particularly the energy dependence of α_I and ρ_{max}) cannot be explained by using atomic wave functions. The inner-shell excitation mechanism proposed by Fano and Lichten¹⁹ may be a more appropriate method in interpreting the experimental results. This mechanism is based upon molecular-orbital (MO) promotion for the limiting case $\eta \ll 1$. The energy of an electron can vary considerably with the internuclear distance r . Levels from different atomic shells can approach closely or even cross at certain critical internuclear distances r_c . At such crossings electron transitions to higher unoccupied levels may occur, and after separation of the collision partners vacancies will be found in inner shells. These crossings can be seen in a diabatic correlation diagram¹⁹; it shows H_2^+ -like correlations between

the atomic levels of two identical atoms at large distances ($r \rightarrow \infty$) and the atomic levels of the united atoms ($r \rightarrow 0$).

L excitation occurs preferentially via the $4f\sigma$ molecular level.¹⁹ In the well-known case Ar-Ar, the $4f\sigma$ level rises steeply at an internuclear distance of about twice the Ar L -shell radius. Kessel³³ assumes the vacancy production $P_I(r_0)$ (r_0 the distance of closest approach) to be an energy-independent step-function: $P_I(r_0) = 0$ for $r_0 > r_c$, and $P_I(r_0) = 2$ for $r_0 < r_c$, since via $4f\sigma$ two electrons are promoted and lost to higher unoccupied shells. This model is reasonably substantiated by large-angle energy loss³⁴ and total x-ray cross section³⁰ measurements in the case of Ar-Ar.

The $P_I(\rho)$ distribution measured for the L -shell vacancy production in the practically symmetric system I-Te shows a somewhat different behavior. (note that distance of closest approach and impact parameter are practically equal, see Fig. 5): (i) $P_I(\rho)$ increases smoothly with decreasing r_0 . No sudden rise of vacancy production is observed. (ii) The maximum number of vacancies created in both particles is appreciably smaller than 2. (iii) $P_I(\rho)$ seems to be energy dependent. A possible energy dependence of the fluorescence yield ω can influence this behavior; however, considering the relatively high value of $\omega_L = 0.14$ it is unlikely that the entire energy dependence is caused by a variable ω_L .

Similar to L excitation in lighter systems the vacancy production occurs within an internuclear distance of about the sum of the L -shell radii of I and Te; it can be neglected for larger distances. These experimental facts may be understood qualitatively from the correlation diagram of, e. g., two Te atoms and a united atom with $Z = 104$.³⁵ The $4f$ level of the united atom Te+Te lies between the $4d$ and the $5s$ level.³⁶ The promotion of the $4f\sigma$ molecular level thus is much less pronounced than in the case Ar-Ar. For small ion velocities, the levels which may interact with $4f\sigma$ are occupied, except possibly $4f\phi$ (rotational coupling¹⁹). The situation is complicated by the collisional smearing of the energy levels which makes the concept of localized crossings ambiguous. Transitions to the higher unoccupied molecular levels and possibly directly into the continuum may occur over a broad range of internuclear distance. In such a way vacancies could be created in some levels before they "cross" $4f\sigma$. A similar mechanism has been discussed for K -shell excitation in Ar-Ar collisions.³⁴ An additional difficulty is introduced by the use of solid targets.^{37,38} The presumption that the higher atomic shells are in the ground state before each collision is not certain to hold true. For the $20\text{-}\mu\text{g}/\text{cm}^2$

Te target single-collision conditions prevail only up to L -shell dimensions (mean free path for a collision involving impact parameters smaller than L -shell radius, $\lambda_L \approx 50 \mu\text{g}/\text{cm}^2$). If the lifetime of an M - or N -shell vacancy is long compared to the ion collision frequency, outer-shell excitation will accumulate while the ion is passing through the target. A molecular level from the L shell will find more unoccupied levels at "crossings," resulting in an enhanced vacancy production.

The effects discussed above may contribute to a lower vacancy production and to a broadening of the effective interaction region, giving rise to the observed gradual increase of $P_I(\rho)$ with decreasing ρ . It can be concluded that in heavier collision systems L -shell excitation cannot be explained by promotion of one or two L electrons at a well-defined internuclear distance. From our experiment it can also be inferred that the high Q values for large-angle scattering found in the quite similar I-Xe collision system³⁹ are only caused to a small extent by L excitation; moreover, the increase in charge state of the scattered I ions⁴⁰ at a distance of about 12×10^{-10} cm is unlikely to be produced by L excitation: No L x rays are observed at that internuclear separations, see Fig. 5. It seems more likely that these processes are mainly caused by multiple M excitation. From the correlation diagram one may expect a large number of M electrons to be promoted. This may be important, e. g., for the detection of superheavy elements by registering their characteristic x radiation in collisions with heavy target atoms. It is expected that only M radiation is excited in the superheavies with sufficiently high cross section.⁴¹

A more sophisticated measurement of the impact-parameter-dependent x-ray production particularly in asymmetric systems, and employing improved x-ray resolution [Si(Li) detectors], should give a further insight into the excitation mechanism. A knowledge of this mechanism will also be a necessity for practical applications of x-ray excitation in heavy-ion-atom collisions.

ACKNOWLEDGMENTS

The authors are deeply indebted to Professor Dr. W. Gentner and Professor Dr. U. Schmidt-Rohr for the hospitality at the Max-Planck Institut fuer Kernphysik, Heidelberg. We are grateful to P. Schmidt, Dr. K. Sistemich, and J. W. Grueter for assistance in the experiments. We thank Dr. K. Reichelt, F. K. Roemer, and H. Wirth for their help with the target preparation, and Mrs. L. Acker and Dr. G. Fiebig for handling the data on the computer.

*Present address: Gesellschaft fuer Schwerionenforschung, Darmstadt, Germany.

¹N. F. Mott and H. S. W. Massey, *The Theory of Atomic Collisions* (Oxford U. P., London, 1965).

- ²E. Merzbacher and H. W. Lewis, in *Handbuch der Physik*, edited by S. Flügge (Springer, Berlin, 1958).
- ³W. Henneberg, *Z. Physik* **86**, 592 (1933).
- ⁴J. Bang and J. M. Hansteen, *Kgl. Danske Videnskab. Selskab, Mat.-Fys. Medd.* **31**, No. 13 (1959); J. M. Hansteen and O. P. Mosebekk, *Z. Physik* **234**, 281 (1970).
- ⁵S. Messelt, *Nucl. Phys.* **5**, 435 (1958).
- ⁶R. C. Jopson and C. D. Swift, *Phys. Rev.* **127**, 1612 (1962).
- ⁷J. M. Khan and D. L. Potter, *Phys. Rev.* **133**, A890 (1964); J. M. Khan, D. L. Potter, and R. D. Worley, *Phys. Rev.* **139**, A1735 (1965).
- ⁸E. Laegsgaard, L. C. Feldman, and J. U. Andersen, in *Abstracts of Papers of the Seventh International Conference on the Physics of Electronic and Atomic Collisions* (North-Holland, Amsterdam, 1971), Vol. 1, p. 414.
- ⁹W. Brandt, R. Laubert, and I. Sellin, *Phys. Rev.* **151**, 56 (1966).
- ¹⁰R. C. Der, T. M. Kavanagh, J. M. Khan, B. P. Curry, and R. J. Fortner, *Phys. Rev. Letters* **21**, 1731 (1968); R. C. Der, R. J. Fortner, T. M. Kavanagh, and J. M. Khan, *Phys. Rev. A* **4**, 2575 (1970).
- ¹¹H. J. Stein, H. O. Lutz, P. H. Mokler, K. Sitemich, and P. Armbruster, *Phys. Rev. Letters* **24**, 701 (1970); H. J. Stein, H. O. Lutz, P. H. Mokler, K. Sitemich, and P. Armbruster, *Phys. Rev. A* **2**, 2575 (1970).
- ¹²W. Brandt and R. Laubert, *Phys. Rev. Letters* **24**, 1037 (1970).
- ¹³M. Terasawa, T. Tamura, and H. Kamada, in Ref. 8, p. 417.
- ¹⁴P. Armbruster, E. Roeckl, H. J. Specht, and A. Vollmer, *Z. Naturforsch.* **19a**, 1301 (1964); H. J. Specht, *Z. Physik* **185**, 301 (1965).
- ¹⁵P. Armbruster, *Z. Physik* **166**, 341 (1962).
- ¹⁶J. A. Cairns, D. F. Holloway, and R. S. Nelson, in *Atomic Collision Phenomena in Solids* (North-Holland, Amsterdam, 1970), p. 541.
- ¹⁷T. M. Kavanagh, M. E. Cunningham, R. C. Der, R. J. Fortner, J. M. Khan, E. J. Zaharis, and J. D. Garcia, *Phys. Rev. Letters* **25**, 1473 (1970).
- ¹⁸F. W. Saris, *Physica* **52**, 290 (1971).
- ¹⁹U. Fano and W. Lichten, *Phys. Rev. Letters* **14**, 627 (1965); W. Lichten, *Phys. Rev.* **164**, 131 (1967).
- ²⁰N. Bohr, *Kgl. Danske Videnskab. Selskab, Mat.-Fys. Medd.* **18**, No. 8 (1948).
- ²¹E. Everhart, G. Stone, and R. J. Carbone, *Phys. Rev.* **99**, 1287 (1955).
- ²²N. Angert, H.-D. Betz, B. Franzke, J. Gučić, E. Leischner, A. Möller, and B. Stadler, *Unilac-Bericht No. 3-67*, University of Heidelberg, 1967, p. 8 (unpublished).
- ²³M. E. Cunningham, R. C. Der, R. J. Fortner, T. M. Kavanagh, J. M. Khan, C. B. Layne, E. J. Zaharis, and J. D. Garcia, *Phys. Rev. Letters* **24**, 931 (1970).
- ²⁴P. H. Mokler, H. O. Lutz, H. J. Stein, and P. Armbruster, *Nucl. Instr. Methods* **90**, 321 (1970).
- ²⁵P. H. Mokler, *Phys. Rev. Letters* **26**, 811 (1971).
- ²⁶S. Datz, C. D. Moak, B. R. Appleton, and T. A. Carlson, *Phys. Rev. Letters* **27**, 363 (1971).
- ²⁷In our previous publications (see Refs. 11 and 24) the quantity $P_I(\rho)$ was named "probability for vacancy production." This notation is only correct if two L vacancies are produced statistically independent as implied by the promotion model (Ref. 19).
- ²⁸E. J. McGuire, *Phys. Rev. A* **3**, 587 (1971).
- ²⁹C. P. Bhalla, *Phys. Rev. A* **2**, 2575 (1970); D. L. Walters and C. P. Bhalla, in Ref. 8, p. 404.
- ³⁰F. W. Saris and D. Onderdelinden, *Physica* **49**, 441 (1970).
- ³¹F. Herman and S. Skillman, *Atomic Structure Calculations* (Prentice-Hall, Englewood Cliffs, N. J., 1963).
- ³²M. Rogge, thesis (University of Heidelberg, 1966) (unpublished).
- ³³Q. C. Kessel, *Bull. Am. Phys. Soc.* **14**, 946 (1969).
- ³⁴See the review article of Q. C. Kessel, in *Case Studies in Atomic Collision Physics* (North-Holland, Amsterdam, 1969), p. 401.
- ³⁵H. J. Stein, Kernforschungsanlage Jülich Report No. JÜL 799/NP, 1971 (unpublished).
- ³⁶Spin-orbit coupling is neglected here. This approximation will suffice for this qualitative discussion.
- ³⁷F. W. Saris and D. J. Bierman, *Phys. Letters* **35A**, 199 (1971).
- ³⁸H. O. Lutz, H. J. Stein, S. Datz, and C. D. Moak, *Phys. Rev. Letters* **28**, 8 (1972).
- ³⁹Q. C. Kessel, P. H. Rose, and L. Grodzins, *Phys. Letters* **22**, 1031 (1969).
- ⁴⁰Q. C. Kessel, *Phys. Rev. A* **2**, 1881 (1970).
- ⁴¹P. Armbruster, P. H. Mokler, and H. J. Stein, *Phys. Rev. Letters* **27**, 7623 (1971).